Full Research Program

Plasmonic Metasurfaces with broken space-inversion symmetry: From geometric Berry phase to topological plasmonics

Gorodetski Yuri

1 Scientific background

Two dimensional (2D) materials have been a subject of great interest for many years, since the discovery of graphene. In recent years the field has developed rapidly with the discovery of many more types of 2D materials such as transition metal dichalcogenide (TMD) monolayers.[1–5] Due to their unique physical properties and potential applications in a wide range of technologies, much research has been devoted to fabrication methods, together with theoretical and experimental studies of their underlying physics. TMDs are semiconductors of the form MX_2 where M is a transition metal atom such as Mo or W and X is a chalcogen atom such as S, Se or Te. It has been shown that these materials, when cleaved to a monolayer, have a direct band-gap and strong spin-orbit coupling, together with favourable electrical and mechanical properties. With these properties, TMDs such as MoS_2 have a valley degree of freedom, enabling the development of valleytronic devices.[6] They also posses topological phases due to their symmetry giving rise to a non-trivial Berry phase and many TMDs behave as topological insulators (TIs) hosting topologically protected conducting edge states.[7,8] Because of the great promise of these materials, further understanding of the physical processes is needed.

The Berry phase[9] is a phase which is added to an eigenstate after completing a closed loop in the parametric space in which it is defined.[10] It is caused by non trivial topology of the state-space and therefore often called a ”geometric phase”.[11,12] In crystals of broken time-reversal or space-inversion symmetry the level degeneracy of the chiral eigenstates (quasi-spins) is lifted giving rise to the so called Berry curvature which can be compared to the appearance of magnetic monopoles.[13] In symmetric structures such as graphene, time-reversal symmetry can be broken using a strong magnetic field. TMDs such as MoS_2 and WSe_2 have a hexagonal lattice structure similar to that of graphene, but unlike the latter, the different atoms within the honeycomb unit cell, break inversion symmetry. Therefore, the Berry phase accumulated by Bloch electrons at their Dirac points, which are degenerate in graphene, are of opposite sign making the K and K’ valleys distinguishable.

It has been repetedly shown that the light modes propagating in a periodically modulated space

can exhibit behavior analogical to electronic wave-function in a crystal.[14,15] The parameter space that defines the state of polarized light is the Poincaré sphere, where the north and south poles correspond to right- and left-hand circular polarization (RCP) and (LCP) respectively. A gradual cyclic change of the polarization state induces a measurable and helicity-dependent Pancharatnam-Berry (PB) phase.[16,17] This phase is equal to half the solid angle enclosed by the loop. The PB phase is responsible for the spin-Hall effect of light[12,18] and has played an important role in numerous applications in optics[19,20] and plasmonics.[21–23]

2 Research objectives and expected significance

Here we consider plasmonic PB phase metasurfaces with graphene-like structures but with broken inversion symmetry. Plasmonic metasurfaces with subwavelength space-variant anisotropic scatterers have been shown to produce the PB phase.[22,24] Such structures have been used for spin-dependant directional excitation of surface plasmon (SP) waves and have been the subject of much research[25–27] due to their potential in development of nano-photonic devices. By measuring the plasmonic response upon illumination with different spin states in momentum space, we show that the excited plasmonic modes strongly depend on the helicity of the incident light. Explicitly, we observe a spin-degeneracy lifting analogous to the behavior of TMDs at their K and K' valleys. In our case, inversion symmetry is broken by angular difference between adjacent apertures in the metasurface. This angle leads to opposite PB phases in the K and K' points in momentum space, resulting in a contrast between the two circular polarizations in both the near and far field. This contrast is then varied by controlling the aperture angle. These results are consistent with numerical calculations that we performed.

Interestingly, it seems that an analogy can be drawn between our structures and 2D materials such as TMDs. Both have a graphene-like structure but with inversion symmetry broken. As mentioned above, this broken symmetry causes a strong spin-orbit interaction and the occurrence of a Berry phase. The plane separation between the constituent atoms in the unit cell can be associated with the rotation of the apertures in our metasurface. The pseudospin accounting for the rotational motion of electrons within the honeycomb unit cell is just like the SP waves circulating in the unit cell of our structure, following the path of constructive phase building. It has been shown that optical topological phases can model complex quantum systems.[28] Much theoretical insight can be gained from such analogies. Although the fabrication of 2D materials is improving rapidly, it currently remains a complicated procedure. Our structures, by contrast, are easy and cheap to pre-

pare, as well as being very flexible having many parameters to play with. Measuring and analysing our system is also very straightforward with many degrees of freedom . We thus propose a simple way to analyze optical properties of TMDs and possibly make predictions of yet unknown features. If this connection could be shown theoretically, this could open many doors to further deepening of our understandings of TMDs.

3 Detailed description of the proposed research and preliminary results

Our metasurface is an array of rectangular apertures in a 100 nm thick gold film, arranged in a honeycomb lattice. The lattice constant is $a = 3\lambda_{sp}/4$, where λ_{sp} is the wavelength of the SP excited at the gold-air interface and is given by $\lambda_{sp} = \frac{2\pi c}{\omega}\sqrt{\frac{1+\epsilon_{Au}}{\epsilon_{Au}}}$, while $\epsilon_{Au}(\omega)$ is the dielectric function of gold at frequency ω. Each two neighboring apertures are rotated such that they have an angle of $\theta = \pi/4$ between them. We used a laser diode at $\lambda_0 = 2\pi c/\omega = 780$ nm and therefore, in our case, $a = 574$ nm. A scanning electron microscope (SEM) image of our sample is presented in Fig. 1 (c). The apertures were milled by using a focused ion beam (FIB), into the gold film that had been evaporated on a glass substrate by sputtering. The laser beam was expanded and then focused by a microscope objective ($NA = 0.25$) on to the sample at the air-gold interface. At the back side, the glass substrate was brought into contact with an oil-immersion objective ($NA = 1.3$) that collected the plasmonic leakage radiation.[29] A tube lens then formed an image on the camera, with an additional (Fourier) lens, on a flipped mount to image the k-space when needed. The polarization state of the incident light was controlled by a set of a polarizer and a waveplate before the sample. The setup is illustrated schematically in Fig. 1 (g). The measurements were preformed both in real and reciprocal (k-space) spaces. In Fig. 1 (a),(b),(d) & (e) the real space distributions for the incident RCP and LCP light, measured with circular analyzer are presented. We clearly see that in the cases of cross-polarization ((b) and (d)) there is a strong localization of light along the circumference of the metasurface, while both the outside and the inside of the structure remain dark. When the output polarization is the same as the input ((a) and (e)) there is no special behaviour and the light seems to be transmitted by the structure. We further measured the response of the structure for both spin states (without polarization filtering at the output) in the k-space and calculated the circular dichroism (CD) of the structure, defined as

$$\Delta = \frac{\sqrt{I_R} - \sqrt{I_L}}{\sqrt{I_R} + \sqrt{I_L}} \tag{1}$$

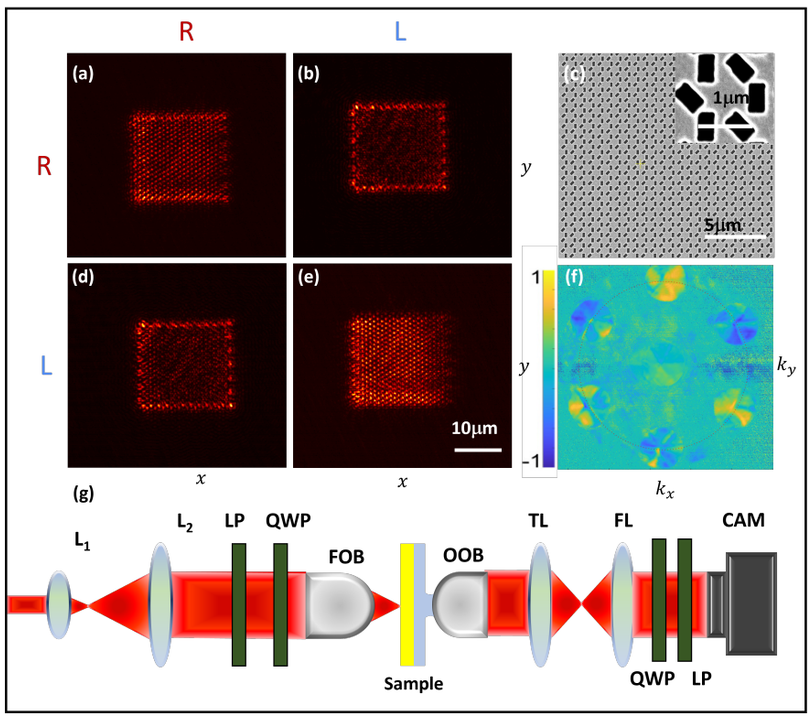

Figure 1: (a),(b),(d) and (e) Plasmonic spin-dependant edge-state at the boundary of a graphene-like metasurface when the output polarization differs from the input (input polarization arranged in rows and output in columns). (c) A SEM image of the metasurface with a close up of the unit cell in the inset. (f) Spatial CD map (in k-space) of the structure. The primary plasmonic resonance circle is marked by the dotted red line. (g) Schematic illustration of the optical setup consisting of lenses (L_1, L_2), a linear polarizer (LP),quater wave plate (QWP), focusing objective (FOB), oil-immersion objective (OOB), tube lens (TL), Fourier lens (FL) and a camera (CAM).

where $I_{R,L}$ is the measured intensity for RCP and LCP illumination, respectively (Fig. 1 (f). K-space measurements will be discussed later in greater detail). We note that the diffraction orders have a strong polarization dependence while the central (zero) order has an almost null CD. Specifically, we observe three predominantly LCP polarized orders while the other three are RCP. This spin-dependent k-space directionality resembles excitonic directional behavior in TMDs.

In order to understand the meaning of these measurements we first refer to the structure discussed in ref. [27]. We consider a hexagonal lattice of rectangular apertures rotating along its primary directions. The rotation rates are defined by constants N = 3 and M = -3 (here N and M are the number of the grating periods needed to complete a rotation of π radians) (see inset in Fig. 2). The relative angle between the neighboring apertures is $\pi/3$ and the lattice constant is $a = 2\lambda_{sp}/3$. As discussed in detail in ref. [27], with these parameters only three unidirectional plasmonic beams are excited for each circular polarization state. This strong polarization selectivity is achieved due to the rotation induced Coriolis term added to the momentum matching condition which leads to the PB phase.

Explicitly, a structure defined by the direct lattice primitive vectors $\mathbf{a} = a\hat{\mathbf{a}}$ and $\mathbf{b} = b\hat{\mathbf{b}}$ produces a diffraction pattern according to its reciprocal primitive vectors $\mathbf{a}^* = 2\pi\frac{\mathbf{b}\times\hat{\mathbf{z}}}{\mathbf{a}\cdot(\mathbf{b}\times\hat{\mathbf{z}})}$ and $\mathbf{a}^* = 2\pi\frac{\mathbf{a}\times\hat{\mathbf{z}}}{\mathbf{a}\cdot(\mathbf{b}\times\hat{\mathbf{z}})}$. However, the space-variant aperture rotation $\theta(x, y)$ (with respect to the y axis) leads to an addi-

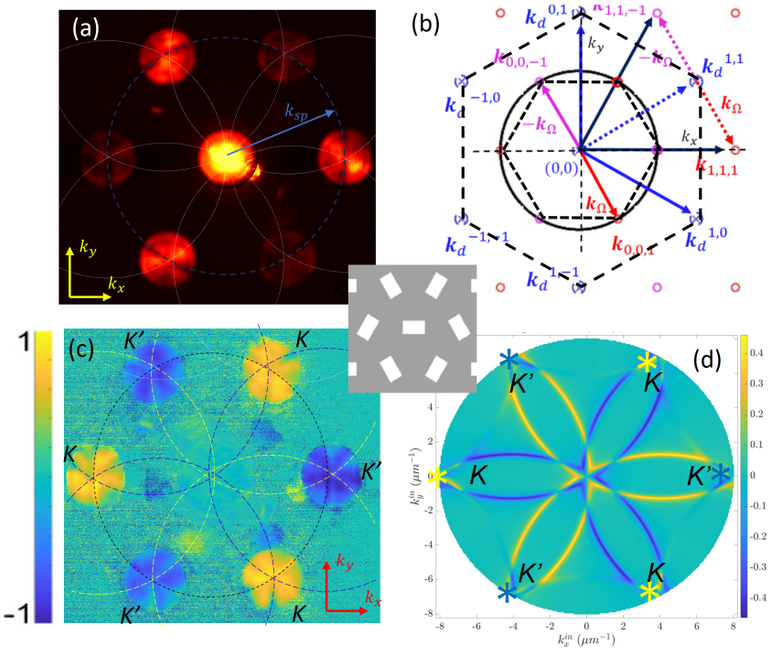

Figure 2: (a) A raw image of our measured angular intensity distribution in an ISF. The primary plasmonic resonance circle marked in blue and the secondary resonances in white. (b) Theoretically calculated k-space diagram. Blue crossed marks correspond to ODOs. Red and lavender circles correspond to RCP and LCP BOs, respectively. Solid blue arrows correspond to the reciprocal lattice vectors and solid red and lavender to the momentum of the two BOs, respectively. Dotted lines show the displacement of an ODO and its respective BOs. Solid dark blue lines denote the total optical momentum of a diffracted mode. (c) CD map of the hexagonal PB phase grating. (d) Simulated CD.

tional term in the total grating momentum of $-\sigma\mathbf{k}_\Omega$. We define the Coriolis term $\mathbf{k}_\Omega = 2\Omega$, where $\Omega = \Omega_\mathbf{a}\hat{\mathbf{a}}^* + \Omega_\mathbf{b}\hat{\mathbf{b}}^*$ is the aperture rotation rate vector, $\Omega_\mathbf{a} = \nabla_\mathbf{a}\theta(x,y) = \frac{\pi}{Na}$ and $\Omega_\mathbf{b} = \nabla_\mathbf{b}\theta(x,y) = \frac{\pi}{Mb}$ are rotation rates along the primary axes and $\sigma = \pm 1$ is the photon spin taking the value $+1$ for RCP and -1 for LCP.

A raw image of the k-space captured by the camera, is presented in figure 2 (a). The k-space image is an isofrequency surface (IFS) which is essentially a slice of the three dimensional dispersion at the laser frequency ω. The diffraction pattern is clearly visible, corresponding to the reciprocal lattice of the hexagonal structure. The circle of radius $|k_{sp}| = 2\pi/\lambda_{sp}$ (marked by the dashed line) is the plasmonic resonance representing the excitation of the SPs at the gold-air interface. The additional circular arcs are replications of the plasmonic momentum circle centered at other diffraction spots, due the grating periodicity.[30] Some of these secondary modes have been marked to guide the eye. Points in k-space at which a diffraction spot coincides with the the primary plasmonic mode represent the particular momentum at which the excitation of the SP occurs. Therefore, in real space, the SPs are seen to propagate in the directions determined by the momentum matching[27] (see Fig. 3 (c)-(f)). As shown schematically in Fig. 2 (b), the diffraction spots coinciding with the plasmonic circle are the Berry orders (BOs), originating from the geometrical phase. The

ordinary diffraction orders (ODOs) which result from the periodicity of the structure (disregarding the rotation of apertures) fall further away and are out of our field of view. The inner hexagonal dashed line marks the edge of the first Brillouin zone (FBZ) with the K and K' points coinciding with BOs. Measuring for both polarization states we obtain the CD map shown in Fig. 2 (c). A close look at the CD map shows that the secondary modes which are centered at the K and K' points maintain the polarization of the corresponding BO. This is seen very clearly in the simulated CD map presented in Fig. 2 (d) in which the plasmonic modes are traced out throughout the entire FBZ using a scattering formalism based on the coupled waveguidemode method.[31] We conclude that the presented hexagonal PB phase structure has a strong spin dependence manifested both in the diffraction pattern and in the secondary plasmonic modes.

Now we consider this hexagonal PB phase structure as a superposition of three sub-lattices of non-rotating apertures, each with a period of $3a$, with a displacement a between them and rotated by 60° with respect to one another, as illustrated in Fig. 3 (a). Obviously, each separate sub-lattice is not expected to induce a PB phase. However, the combination of the three structures at different orientations gives rise to the PB phase as discussed above. Yet, when one of the sub-lattices is removed the resulting structure becomes a graphene-like metasurface with lattice constant $a = 2\lambda/3$ and relative angle $\theta = \pi/3$, as shown in Fig. 3 (b). It should now be pretty obvious that the efficiency of the full hexagonal structure is degraded and the spin-degeneracy that was lifted, reappears. Nevertheless, the broken space-inversion symmetry of the structure is still results in spin-dependent directionality. Both real and k-space measurements of such a structure are presented in Fig. 3 (c)-(f) showing the described behaviour.

One may link the weaker polarization contrast to the PB phase discontinuity due to the missing sub-lattice. This can be then compensated by varying the relative angle between the two remaining sub-lattices. We fabricated several more structures with different relative angles and measured the CD maps in the k-space (Eq. 1). From the CD we calculated the polarization contrast between the orders at the points K and K' and plotted it versus the relative angle α (see Fig.4 a). For the comparison we used a simple model based on Huygens principle to simulate the momentum space distribution of the SP waves excited by the sub-lattices with a phase difference of $2\sigma\theta(x, y)$ (dashed line in Fig.4 a).

It can be seen in the full range of the scanned angles (from 0° to 90°) the the measured points show qualitative correspondence to the model prediction with a peak contrast around 33°. When the relative angle tends to 0° or 90° the structure becomes spin-degenerate (as expected) and the

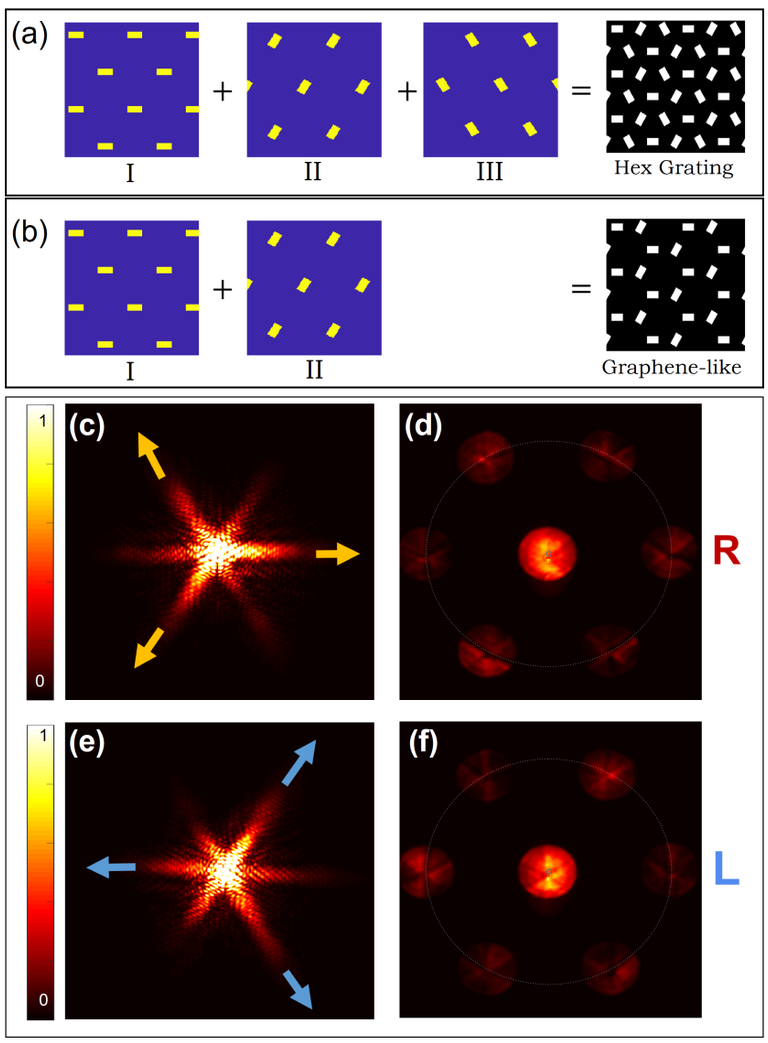

Figure 3: (a) Illustration of decomposition of the hexagonal topological grating into three topologically trivial sub-lattices. (b) Superposition of only two sub-lattices gives our graphene-like metasurface. Correspondence between k-space and real space. (c),(d) Real and k-space images respectively for RCP light. The three brighter diffraction spots coinciding with the plasmonic circle in (d) correspond to the three stronger plasmonic beams propagating in real space in (c). (e) and (f) The same as (c) and (d) for LCP light.

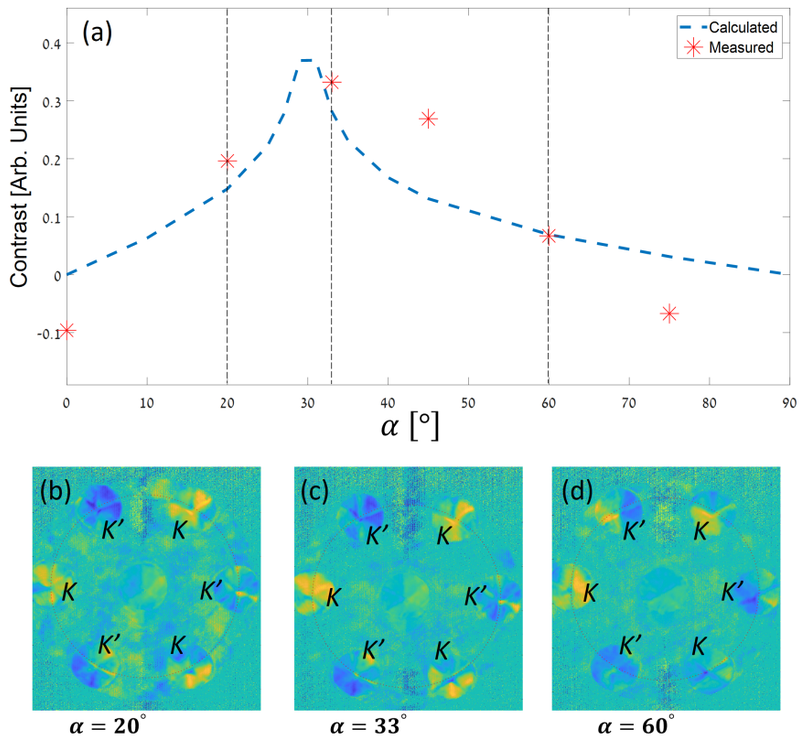

Figure 4: (a) Measured intensity contrast between diffraction orders excited with different circular polarizations as a function of the relative angle between the two sublattices. (b)-(d) Measured k-space CD maps for angles $20°, 33°, 60°$.

polarization contrast diminishes. This confirms that indeed the PB phase acquired by the SP waves is the main effect responsible for the spin-dependent directional excitation in our graphene-like metasurface. Again, this polarization selectivity in the K and K' directions is reminiscent of the spin-dependent valleys in the characteristic dispersion of the TMDs. Further important observations can be made by investigating the particular CD maps of structures with different α (Fig.4 (b)-(d)). We see that the structure with $\alpha = 33°$ exhibiting the maximum contrast (Fig. 4 (c)) is also characterized by rather homogeneous diffraction spots, similar to the hexagonal structure in Fig.2 (c). Moving away from the peak angle we note that the polarization of the orders located at K and K' points become space-variant. Interestingly, this behaviour is also imprinted in the corresponding plasmonic modes. Figure 5 (a) shows the measured and the calculated IFS CD map behind the structure with a lattice constant $a = 510$ nm and $/theta = \pi/3$. It appears from the color-coding that the polarization exciting each of the plasmonic mode rings is strongly varying along the azimuthal direction. This effect becomes even more pronounced when the structure period is increased to $a = 574nm$ (see Fig. 1) and the angle is set to $\theta = \pi/4$. The measured and the calculated maps indicate the polarization state of the absorption in the k-space, therefore one can regard our structure as a resonant space-variant polarizer. The effect of this optical manipulation is conveniently mapped as a closed path on a Poincaré sphere resulting in the geometric Berry phase. By following the calculated plasmonic modes one can indeed notice a winding phase within each diffraction spot

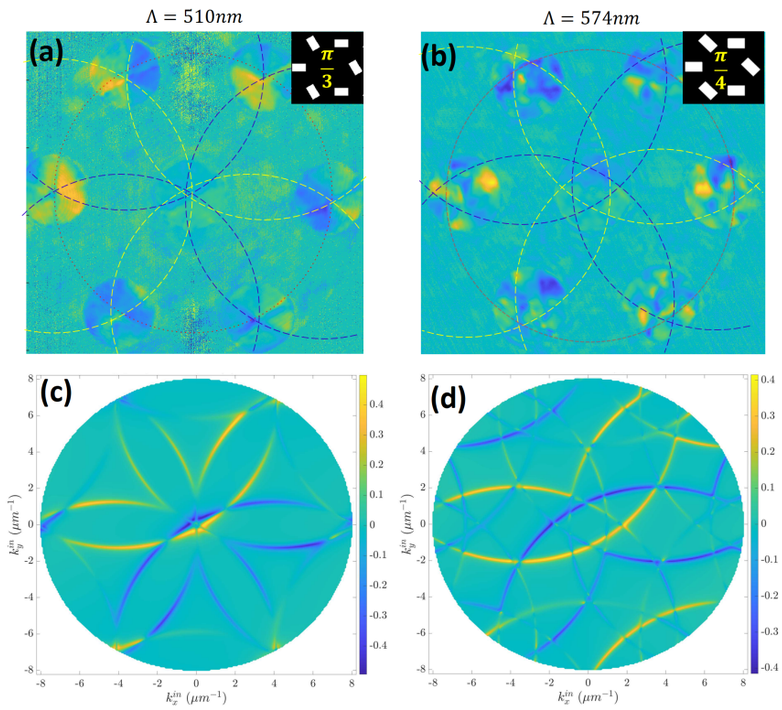

Figure 5: Measured CD maps in of graphene-like structure with a lattice constant $a = 510$ nm (a) and $a = 574$ nm (b) showing space-variant polarization. (c) and (d) Simulated CD maps for given periods.

which appears to be a function of structure period and the relative angle. When we now turn to the raw k-space images measured with the latter structures ($a = 574nm$ and $\alpha = \pi/4$) we can recognize a dark spot in the center of each diffraction spot resulted as we believe from the aforementioned phase singularity. We compare this distribution with the one measured from the full hexagonal structure but illuminated with a laser beam decorated by a spiral phase (see Fig.6). The similarity between the images leads us to the conclusion that our graphene-like structure shown in Fig. 1 induces an optical vortex in each diffraction order.

3.1 Working Hypothesis

It appears that turning a hexagonal structure into a graphene-like structure by subtracting one of the three comprising sub-lattices makes a fundamental change in the behavior of the SPs. First, as can be seen in Fig. 6 each of the 6 apertures in a graphene-like unit-cell has now only three neighbours in a contrast with 6 neighbours in the hexagonal one. This clearly reduces the plasmonic hopping mobility in the array leading to band-gap opening along the primary axes. Accordingly, the SP wave is forced to circulate between the closest neighbours in the unit-cell. When the apertures of the array are rotated, the unit-cell becomes chiral, which lifts the degeneracy between the two counter circulating plasmonic modes, giving rise to a favourable vorticity. Summing up the local unit-cell bound SP vortices results in our case in an overall topological Berry phase along the edge of the whole structure seen in Fig. 1 as an edge state. This polarization dependent plasmonic

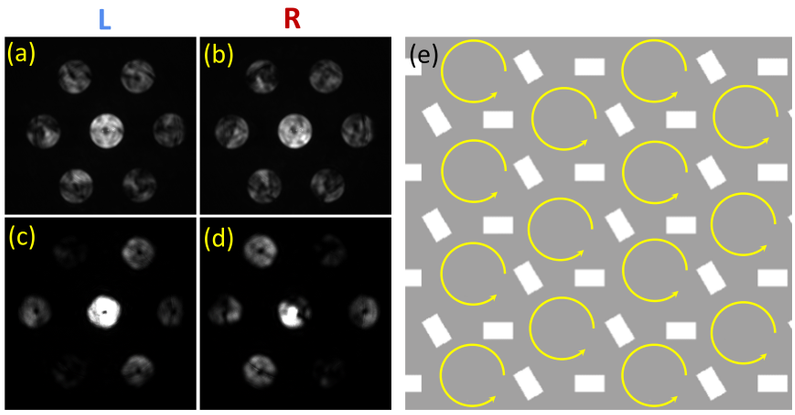

Figure 6: The comparison of the measured k-space distributions for the structure with $a = 574$ nm and $\alpha = \pi/4$ with RCP and LCP illumination (a) and (b) and for the hexagonal structure decorated with a spiral phase with $a = 510$ nm with RCP and LCP illumination (c) and (d). The schematic plasmonic hopping circulation is shown in (e).

mode is induced by a space-inversion symmetry breaking in the structure in analogy with a variety of recently presented topological insulators.

3.2 Research design and methods

The research plan suggests theoretical modelling of the plasmonic metasurface based on the concepts of topological photonics and analogies with TMD behavior. Initially, a geometry and the structure parameters are chosen depending on the desired functionality. Then a numerical model is investigated using a commercially available software (such as Comsol Multiphysics and Lumerical) and also by semi-analitical methods based on the scattering formalism.[31] Once the metasurface is optimized it is designed and fabricated on a thin (100 nm) golden layer by means of a FIB milling. We use sputtering type evaporation to avoid homogeneity caused by large scale crystallization. The analysis of the structure is then performed in a free-space beam set-up shown in Fig. 1 under illumination of a CW diode laser at the wavelength of 780 nm. The polarization state at the entrance and the exit of the system is controlled by a set of the HWP and a QWP. The k-space images are obtained by an additional Fourier lens. The CD maps are acquired using the Eq. 1 by alternate illumination with the RCP and the LCP states.

3.3 Future plan and outlook

Our preliminary results show that space-inversion symmetry in graphene-like plasmonic metasurfaces leads to strong polarization dependent directivity of SP modes and under some conditions result in a spin-dependent edge state. This effects have been recently demonstrated with excitonic modes in TMDs. We believe that further study of our proposed structures may shed light on the

fundamental aspects of topological phases both in solid state physics and in photonics providing a vast range of possible nanophotonic applications. The main aim of the proposed research is to establish our experimental findings by a solid theoretical modelling as well as explore the variety of designs and concepts of topological plasmonic metasurfaces. Specifically, the future research will be concentrated on the following subjects:

- Direct measurement of the topological phase Preliminary results show that our structure is capable of inducing a spiral phase due to a space-variant coupling to the plasmonic modes. Currently this effect has been only shown quantitatively by comparing with the hexagonal structure illuminated with a spiral phase (see Fig.6). Nevertheless, this phase can be measured in our system by using heterodyne interferometry. Previously we have constructed a leakage radiation microscopy set-up embedded in a Mach–Zehnder interferometer in order to obtain an instantaneous phase of a plasmonic signal (see Fig. 7). This system has been

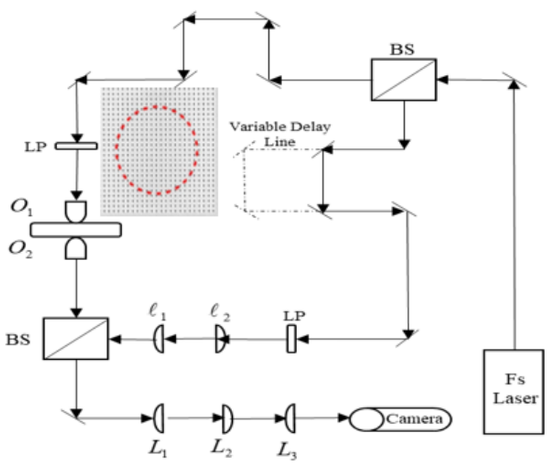

Figure 7: Hetrodyne system based on a Mach-Zehnder interferometry for time-resolved plasmonic pulse tracking.

earlier used to track the propagation in time of ultra-short plasmonic pulses.[32] We propose to modify this set-up in order to conveniently capture the phases of different diffraction orders in the k-space. These measurements can provide the connection between the structure configuration and geometry and the resulting topological phases.

- **Developing a rigorous mathematical model of topology based plasmonic manipulation** We plan to elaborate a theoretical basis of the proposed effect starting from an accurate analysis of the band-gap characteristics, studying the geometrical effects and optimizing the system. The developed model should directly link the physical grating parameters with the localization strength and the lifetime of plasmonic edge modes.

- **Realizing topological metasurface based on graphene-like structure** We propose to in-

vestigate more plasmonic structures potentially leading to the appearance of edge states, topological phases and spin-dependent behavior. Using the space-inversion symmetry as a trigger for spin-orbit coupling in the system we propose using arrays with chiral unit-cells (see Fig. 8. We believe that the chirality would have an effect on the overall topological phase of the domain and, consequently, may provide an additional means for light manipulation. Specifically we believe that each unit cell of the structure induces chiral plasmonic near-fields that may result in an ovelall topological phase. Similar structures with constant or space-variant chirality, already investigated in our group, have shown strong polarization dependent behavior and may be good candidates for topology based plasmonics.[33]

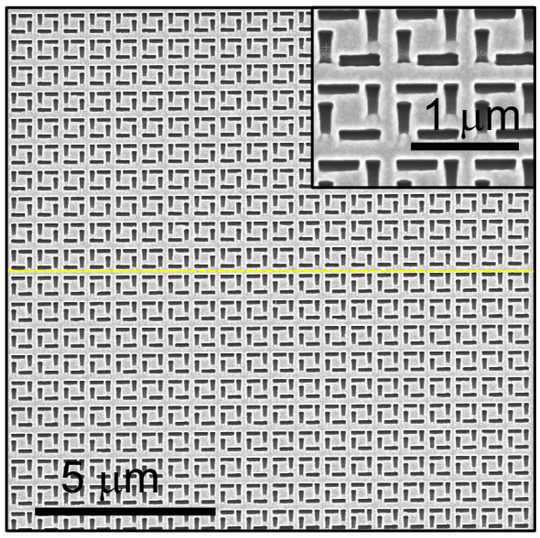

Figure 8: SEM image of the fabricated chiral metasurface. The unit cell here comprises of 4 rectangles arranged in a chiral way with a broken mirror symmetry (see the inset). The handedness of the unit cell in the upper part is opposite to the one in the lower part (a dashed line separates the domains).

We intend to investigate the behavior of plasmonic waves in structure ”domains” with opposite handedness, that could lead to the topological states.

- **Proposing practical applications** Some practical applications for sensing, optical communication, computing and nanophotonic circuitry will be proposed and experimentally tested. We believe that the proposed plasmonic metasurfaces and the fundamental concepts can play a crucial role in understanding of complex physical mechanisms that govern the optical spin-orbit interaction and topological photonics as well as opening new opportunities in nanotechnology development.

3.4 Current research infrastructure

Our nanooptics lab in Ariel University posses the following equipment

- High Resolution Sputter Coater equipped with QCM thickness meter – for gold evaporation
- Preheated sonication bath – for sample and glassware cleaning
- Drying oven (250l) with air circulation mechanism – for drying samples
- Pigtail CW laser ($\lambda_0 = 780nm$, 20mW power)
- C-Fiber 780 femtosecond Erbium laser ($\lambda_0 = 780nm$, $70fspulseduration$ 100mW average power)
- Polarizing elements – for full polarization control
- Optics free space elements – for beam shaping filtering aligning and manipulating
- Number of CMOS and CCD based cameras – for image acquisition
- Computers – for collecting data and controlling the optical elements
- Various PZT based transducers and motors – for precise alignment
- Optomechanical elements
- Olympus microscope
- Optical dry and oil immersion objectives – for imaging and illumination of samples
- Three TMC air damped and stabilized optical tables
- One computer station with COMSOL software installed on it

Resources outside of Ariel University

- Bar-Ilan university nanofabrication facilities – for nanofabrication of our samples
- Tel-Aviv university nanofabrication facilities – for nanofabrication of our samples

Human resources currently affiliated with the project

- Eliav Epstein – research fellow (Graduated with PhD, January 2021)
- Pasha Goz – PhD student (finishes February 2027)
- Sahil Sahoo – PhD student (finishes October 2027)

3.5 Expected Outcomes and Pitfalls

We start with the investigation of SP wave propagation in lattices with broken space-inversion symmetry as discussed in previous sections. While the preliminary results are convincing, more experimental data should be obtained in order to verify our concepts and conclusions. In particular we plan to perform a full numerical study of the photonic band-gap structure of our metasurfaces and compare the results obtained with graphene-like unit-cell and the hexagonal structure. By manipulating with the periodicity, orientation angle and other parameters we plan to achieve various topological phases in K and K' points. This could provide a means for topological based plasmonic mode manipulation. We expect to summarize our results and further investigations in 7 to 9 high-impact factor papers within the period of the three years.

Although some of the expected results have been partially verified in our lab the future investigation will have to deal with rather complex experimental settings and nanofabrication challenges. We have much experience in both of these areas, nevertheless we take into account possible pitfalls that could arise from either technical or theoretical issues. With this in mind we expect that this research could provide a fundamental niche for further studies in topological plasmonics and nanophotonics in general.

Bibliography

[1] N. Mounet, M. Gibertini, P. Schwaller, D. Campi, A. Merkys, A. Marrazzo, T. Sohier, I. E. Castelli, A. Cepellotti, G. Pizzi, *et al.*, “Two-dimensional materials from high-throughput computational exfoliation of experimentally known compounds,” *Nature nanotechnology*, vol. 13, no. 3, pp. 246–252, 2018.

[2] S. Z. Butler, S. M. Hollen, L. Cao, Y. Cui, J. A. Gupta, H. R. Gutiérrez, T. F. Heinz, S. S. Hong, J. Huang, A. F. Ismach, *et al.*, “Progress, challenges, and opportunities in two-dimensional materials beyond graphene,” *ACS nano*, vol. 7, no. 4, pp. 2898–2926, 2013.

[3] S. Manzeli, D. Ovchinnikov, D. Pasquier, O. V. Yazyev, and A. Kis, “2d transition metal dichalcogenides,” *Nature Reviews Materials*, vol. 2, no. 8, pp. 1–15, 2017.

[4] G. Wang, A. Chernikov, M. M. Glazov, T. F. Heinz, X. Marie, T. Amand, and B. Urbaszek, “Colloquium: Excitons in atomically thin transition metal dichalcogenides,” *Reviews of Modern Physics*, vol. 90, no. 2, p. 021001, 2018.

[5] A. Gupta, T. Sakthivel, and S. Seal, “Recent development in 2d materials beyond graphene,” *Progress in Materials Science*, vol. 73, pp. 44–126, 2015.

[6] J. R. Schaibley, H. Yu, G. Clark, P. Rivera, J. S. Ross, K. L. Seyler, W. Yao, and X. Xu, “Valleytronics in 2d materials,” *Nature Reviews Materials*, vol. 1, no. 11, pp. 1–15, 2016.

[7] F. Wu, T. Lovorn, E. Tutuc, I. Martin, and A. MacDonald, “Topological insulators in twisted transition metal dichalcogenide homobilayers,” *Physical review letters*, vol. 122, no. 8, p. 086402, 2019.

[8] X. Li, S. Zhang, and Q. Wang, “Topological insulating states in 2d transition metal dichalcogenides induced by defects and strain,” *Nanoscale*, vol. 9, no. 2, pp. 562–569, 2017.

[9] M. V. Berry, “Quantal phase factors accompanying adiabatic changes,” *Proceedings of the Royal Society of London. A. Mathematical and Physical Sciences*, vol. 392, no. 1802, pp. 45–57, 1984.

[10] D. Xiao, M.-C. Chang, and Q. Niu, “Berry phase effects on electronic properties,” *Reviews of modern physics*, vol. 82, no. 3, p. 1959, 2010.

[11] J. Segert, “Photon berry’s phase as a classical topological effect,” *Physical Review A*, vol. 36, no. 1, p. 10, 1987.

[12] K. Y. Bliokh, A. Niv, V. Kleiner, and E. Hasman, “Geometrodynamics of spinning light,” *Nature Photonics*, vol. 2, no. 12, pp. 748–753, 2008.

[13] L. Lu, J. D. Joannopoulos, and M. Soljačić, “Topological photonics,” *Nature photonics*, vol. 8, no. 11, pp. 821–829, 2014.

[14] J. D. Joannopoulos, P. R. Villeneuve, and S. Fan, “Photonic crystals,” *Solid State Communications*, vol. 102, no. 2-3, pp. 165–173, 1997.

[15] E. Yablonovitch, “Inhibited spontaneous emission in solid-state physics and electronics,” *Physical review letters*, vol. 58, no. 20, p. 2059, 1987.

[16] S. Pancharatnam, “Generalized theory of interference and its applications,” in *Proceedings of the Indian Academy of Sciences-Section A*, vol. 44, pp. 398–417, Springer, 1956.

[17] M. V. Berry, “The adiabatic phase and pancharatnam’s phase for polarized light,” *Journal of Modern Optics*, vol. 34, no. 11, pp. 1401–1407, 1987.

[18] K. Y. Bliokh and Y. P. Bliokh, “Topological spin transport of photons: the optical magnus effect and berry phase,” *Physics Letters A*, vol. 333, no. 3-4, pp. 181–186, 2004.

[19] C. McDonnell, J. Deng, S. Sideris, T. Ellenbogen, and G. Li, “Functional thz emitters based on pancharatnam-berry phase nonlinear metasurfaces,” *Nature communications*, vol. 12, no. 1, pp. 1–8, 2021.

[20] S. Liu, S. Qi, Y. Li, B. Wei, P. Li, and J. Zhao, “Controllable oscillated spin hall effect of bessel beam realized by liquid crystal pancharatnam-berry phase elements,” *Light: Science & Applications*, vol. 11, no. 1, p. 219, 2022.

[21] Z. Bomzon, G. Biener, V. Kleiner, and E. Hasman, “Space-variant pancharatnam–berry phase optical elements with computer-generated subwavelength gratings,” *Optics letters*, vol. 27, no. 13, pp. 1141–1143, 2002.

[22] K. Y. Bliokh, Y. Gorodetski, V. Kleiner, and E. Hasman, “Coriolis effect in optics: unified geometric phase and spin-hall effect,” *Physical review letters*, vol. 101, no. 3, p. 030404, 2008.

[23] K. Y. Bliokh, “Geometrical optics of beams with vortices: Berry phase and orbital angular momentum hall effect,” *Physical Review Letters*, vol. 97, no. 4, p. 043901, 2006.

[24] Y. Gorodetski, A. Niv, V. Kleiner, and E. Hasman, “Observation of the spin-based plasmonic effect in nanoscale structures,” *Physical review letters*, vol. 101, no. 4, p. 043903, 2008.

[25] L. Huang, X. Chen, B. Bai, Q. Tan, G. Jin, T. Zentgraf, and S. Zhang, “Helicity dependent directional surface plasmon polariton excitation using a metasurface with interfacial phase discontinuity,” *Light: Science & Applications*, vol. 2, no. 3, pp. e70–e70, 2013.

[26] J. Lin, J. B. Mueller, Q. Wang, G. Yuan, N. Antoniou, X.-C. Yuan, and F. Capasso, “Polarization-controlled tunable directional coupling of surface plasmon polaritons,” *Science*, vol. 340, no. 6130, pp. 331–334, 2013.

[27] M. Fox and Y. Gorodetski, “Generalized approach to plasmonic phase modulation in topological bi-gratings,” *Applied Physics Letters*, vol. 120, no. 3, p. 031105, 2022.

[28] L. Feng, R. El-Ganainy, and L. Ge, “Non-hermitian photonics based on parity–time symmetry,” *Nature Photonics*, vol. 11, no. 12, pp. 752–762, 2017.

[29] A. Drezet, A. Hohenau, D. Koller, A. Stepanov, H. Ditlbacher, B. Steinberger, F. R. Aussenegg, A. Leitner, and J. R. Krenn, “Leakage radiation microscopy of surface plasmon polaritons,” *Materials science and engineering: B*, vol. 149, no. 3, pp. 220–229, 2008.

[30] E. D. Epstein, L. Singh, S. Sternklar, and Y. Gorodetski, “The role of plasmonic excitations in the optical activity of periodic structures with configurational chirality,” *Applied Physics Letters*, vol. 116, no. 13, p. 131106, 2020.

[31] F. Lorén, G. L. Paravicini-Bagliani, S. Saha, J. Gautier, M. Li, C. Genet, and L. Martín-Moreno, “Microscopic analysis of spin-momentum locking on a geometric phase metasurface,” *Physical Review B*, vol. 107, no. 16, p. 165128, 2023.

[32] Y. Gorodetski, T. Chervy, S. Wang, J. A. Hutchison, A. Drezet, C. Genet, and T. W. Ebbesen, “Tracking surface plasmon pulses using ultrafast leakage imaging,” *Optica*, vol. 3, no. 1, pp. 48–53, 2016.

[33] L. Singh, M. Fox, S. Sternklar, and Y. Gorodetski, “Topological diffraction from grating with space variant chirality,” *ACS Photonics*, vol. 9, no. 4, pp. 1395–1399, 2022.